10

Controlled phase wafers based on inhomogeneously anisotropic nematic liquid crystals

© L.S. Aslanyan, A.E. Aivazyan

Yerevan State University, Yerevan, Armenia

e-mail: leon@ysu.am

Received May 20, 2025
Revised September 15, 2025
Accepted September 16, 2025

The peculiarities of polarized light propagation in a thin layer of nematic liquid crystal in the presence of an electrostatic field that perturbs the uniform distribution of the director (unit vector parallel to the local optical axis) are considered. The analysis is conducted using the quasi-isotropic approximation of geometric optics. From unified positions, approximate equations, their solutions, and analytical expressions for the Stokes parameters are obtained. Using these expressions, the spatial evolution of light polarization inside the sample, the dependence of the output light polarization state on the applied field strength, and the potential applications of such controllable phase plates of various types are analyzed.

Keywords: light polarization, nematic liquid crystals.

DOI: 10.61011/EOS.2025.09.62307.8190-25

1. Introduction

The critical role of light polarization in modern optics and photonics is hard to overestimate. Polarization elements are essential in interferometers and light modulators, in spectroscopy, lasers, and laser systems. In nonlinear optics, polarization methods are crucial for phase-matching processes and for analyzing tensor properties of nonlinear optical susceptibilities of different orders. Light polarization is also important for liquid crystals (LCs), which are part of everyday life [1–3].

In modern optoelectronics and photonics, various media are used for optical elements controlling light polarization state (phase plates or phase retardation elements). These include pure and doped LCs, periodic media with metallic and dielectric coatings, anisotropic and bianisotropic media, etc.

To significantly expand the capabilities of such phase plates and their applications in various controllable elements, media with induced anisotropy inhomogeneity are employed. Control of these systems can be done via electric, magnetic, acoustic, or optical fields [4–8]. One of the easily controllable elements is pure and doped LC structures. Reorientation of the nematic liquid crystal (NLC) director causes redistribution of the LC optical axis throughout the bulk, i.e., local anisotropy inhomogeneity. From a practical standpoint, the ability to externally control such anisotropy inhomogeneity is important. For example, in [9] the peculiarities of light reflection and refraction in LC media under electric field were studied, with a detailed description of effects related to turning points that lead to band gaps, mode transformations, tunneling effects, and over-barrier reflection. Reference [10] explored electric field influence on local director orientation, accompanied by changes in the cell's electric capacitance. Note that this capacitance method (measuring the LC cell capacitance under various voltages) is used to study dielectric and magnetic properties of NLCs.

The present work aims to theoretically analyze the influence of inhomogeneous director distribution on the spatial evolution of light polarization by the quasi-isotropic approximation (QIA) of geometric optics (GO) [11,12] and, based on obtained results, to consider possibilities for their use as controllable phase plates of various purposes.

2. System of Equations in the Quasi-Isotropic Approximation

In the NLCs considered below, anisotropy inhomogeneities induced by external fields most frequently occur. For concreteness, we will only discuss the case of electrostatic field, since the induction mechanism of anisotropy inhomogeneity is unimportant. Obviously, the induced anisotropy inhomogeneity strongly affects light wave propagation in such a medium. Consequently, analyzing the evolution of light polarization when propagating in such an inhomogeneously anisotropic medium is relevant. Although this task is well studied, including by GO, here we apply another method the quasi-isotropic approximation (QIA) of GO [11,12], which allows presenting the analytical solution in a more symmetric and analysis-friendly form. Previously, this method was applied to LCs with twist orientation ([13–17] and references therein).

We study the propagation of a plane monochromatic wave in a nonabsorbing layered inhomogeneous anisotropic medium. As such a medium, consider a homeotropically oriented NLC with anisotropy inhomogeneity created by an electrostatic field [18]. Given the small thickness

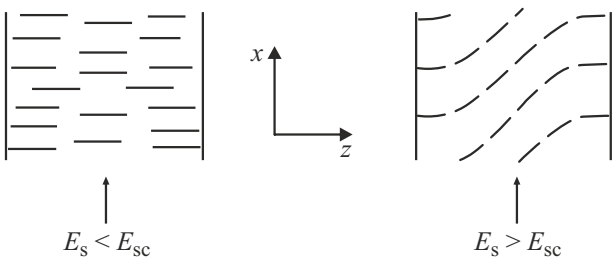

Figure 1. Director distribution under the Fredericks effect.

of the NLC layer, beam curvature during propagation can be neglected (i.e., neglecting the longitudinal electric field component arising from director deformation). The laboratory coordinate system is chosen so that the z axis coincides with the wave propagation direction. The x axis is co-directional the external electrostatic field, and the y-axis is perpendicular to the xz plane so that x, y, z completes a right-handed coordinate system (Fig. 1). Usually, the wave equation is reduced to a two-dimensional form for such problems ([14–17] and references therein). In the case of normal incidence on such a medium (parallel to z) axis), the two-dimensional wave equation for components E_x and E_y has the form

$$\left\{ \begin{array}{l} \frac{d^2E_i(z)}{dz^2} + \frac{\omega^2}{c^2}h_{ij}(z)E_j(z) = 0, \\ i, j = x, y. \end{array} \right\} \qquad (1)$$

The two-dimensional tensor h_{ij},

$$h_{ij}(z) = \varepsilon_{ij} - \frac{\varepsilon_{iz} - \varepsilon_{jz}}{\varepsilon_{zz}}, \qquad (2)$$

is directly connected to the three-dimensional dielectric permittivity tensor and characterizes the optical properties of the medium. As is well known, the dielectric permittivity of NLC is expressed as

$$\varepsilon_{ij} = \varepsilon_o\delta_{ij} + \varepsilon_a m_i(z)m_j(z),$$

where $m_i(z)$ are the director components describing the local optical axis orientation, δ_{ij} is the Kronecker delta symbol, $\varepsilon_a = \varepsilon_e - \varepsilon_o$ is the NLC anisotropy, and ε_e, ε_o are the principal values of the ε_{ij} tensor [18]. In the structures considered below, the director deformation occurs in the xz plane, i.e.,

$$\mathbf{m}(z) = \{\sin\theta(z), 0, \cos\theta(z)\}, \qquad (2a)$$

where θ is the angle between the director direction and the $z$axis. In many important problems involving layered inhomogeneous media, dielectric permittivity $\varepsilon_{ij}(z)$ is a smoothly varying function along axis $z$justifying the use of approximate methods, in particular GO. Indeed, GO approximation is applicable if $\lambda d\varepsilon/dz \ll \varepsilon$ [11]. For example, for light waves in NLC MBBA ($\varepsilon_e = 3.22$; $\varepsilon_0 = 2.43$,[18]) this condition is satisfied when $L \gg 0.4\,\mu$m, where L is the LC layer thickness, i.e., practically always. In the quasi-isotropic approximation (QIA) an additional requirement arises. QIA is based on the assumption that the electromagnetic field in the zero approximation has a transverse structure as in the isotropic case, i.e., the anisotropy tensor

$$\nu_{ik} = h_{ik} - \varepsilon\delta_{ik}$$

also satisfies the smallness condition: $\max|\nu_{ik}| \ll 1$, where

$$\varepsilon = \frac{1}{2}Sph_{ik}$$

is the isotropic part of the tensor h_{ik} [12]. It is easy to verify that for NLC MBBA this condition is also satisfied (for example, $\nu_{xx}/\varepsilon \sim 0.1$).

We seek the solution of the two-dimensional wave equation (1) in the form

$$E_i(z) = \frac{J_i(z)}{\sqrt{\phi'(z)}}\exp\left\{i\frac{\omega}{c}\Phi(z)\right\}. \qquad (3a)$$

The justification for such form is given in [14]. Here $J_i(z)$ is a slowly varying complex amplitude. The phase factor $\Phi(z)$ has the form

$$\Phi(z) = \int n(z)dz = \int \sqrt{\varepsilon(z)}dz. \qquad (3b)$$

$$n^2(z) = \varepsilon(z) = \frac{1}{2}Sph_{ik}(z). \qquad (3c)$$

After substituting (3a) into (1), neglecting J_i'' (according to GO method) and considering (2), we obtain

$$\frac{dJ_i(z)}{dz} = i\frac{\omega}{c}\frac{h_{xx} - h_{yy}}{4n(z)}\sigma_{1ij}J_j(z), \qquad (4)$$

where $\hat{\sigma}_1$ is the Pauli matrix:

$$\hat{\sigma}_1 = \begin{pmatrix} 1 & 0 \\ 0 & -1 \end{pmatrix}.$$

The resulting system of equations (4) completely describes the propagation of a polarized wave in an inhomogeneous anisotropic medium.

3. Solution of equations in inhomogeneous anisotropic NLC

For the final analytical solution of the problem, the distribution $\theta(z)$ must be specified. Let us discuss a particular example. Consider the case when director deformation in the x, z plane is created by a transverse electrostatic field (the so-called Fredericks effect) (Fig. 1). In liquid crystal physics, the Fredericks transition refers to the director reorientation under external electric, magnetic, or optical fields [19] It is well studied both experimentally and theoretically. Under rigid boundary conditions that is,

when $\theta(0) = \theta(d) = 0$ (d the cell thickness), the director distribution is described by the formula [18]

$$\theta(z) = 2\sqrt{\frac{E_s}{E_{sc}} - 1}\sin\left(\frac{\pi z}{d}\right). \qquad (5)$$

Here E_s -is the strength of the applied electrostatic field on the cell, E_{sc} its critical value, above which reorientation occurs. As seen from (5), by adjusting the ratio E_s/E_{sc} one can ensure the condition $\theta(z) \ll 1$making the use of GO justified. It is easy to verify that in this approximation $n(z) \approx \sqrt{(\varepsilon_o)}$ (according to (3c)). From (4), it is also easy to notice that in the case of deformation in the x, z plane, the system splits into two independent equations. Then the solution of equations (4) can be straightforwardly represented using (2) and (3) in the form

$$E_i(z) = \frac{A_i}{\sqrt{\varepsilon_o}}\exp\left\{i\frac{2\pi}{\lambda} \times \left[\Phi(z) + i(\hat{\sigma}_1)_{ii}\frac{\varepsilon_a\sqrt{\varepsilon_o}}{4\varepsilon_e}\int\theta^2(z)dz\right]\right\}. \qquad (6)$$

Integration constants A_i are determined from boundary conditions

$$E_x(0) = \cos\beta_0, \qquad E_y(0) = \sin\beta_0 e^{i\delta_0},$$

where β_0 is the azimuthal angle of the incident linearly polarized wave, and δ_0 is the initial wave phase offset if the incident wave is elliptically polarized. The intensity is normalized to unity. Substituting (5) into (6) and evaluating the integral, taking into account the boundary conditions, the final solution can be expressed as follows:

$$E_i(z) = E_i(0)\exp\left\{i\frac{2\pi\sqrt{\varepsilon_o}}{\lambda}[z + \varphi(z)\sigma_{1ii}]\right\}, \qquad (7)$$

$$\varphi(z) = \frac{\varepsilon_a}{2\varepsilon_e}\left(\frac{E_s}{E_{sc}} - 1\right)\left(z - \frac{d}{2\pi}\sin\frac{2\pi z}{d}\right).$$

Expression (7) is the final analytical solution for the Fredericks transition problem. Note that unlike previously obtained results, it has a relatively simple and convenient form for analysis and practical use.

4. Discussion

A convenient way to visually describe the spatial evolution of polarization of light propagating in the medium is on the Poincare sphere, where points correspond uniquely to light polarization states. The coordinate axes of the Poincare sphere are formed by components of the Stokes vector: [19]:

$$\mathbf{S}(z) = \mathbf{E}^+(z)\hat{\sigma}\mathbf{E}(z), \qquad (8a)$$

where $\hat{\sigma}_i$ are the Pauli matrices. Using (7) and (8a), analytical expressions for the Stokes parameters can be readily found:

$$(S_1(z) = \cos(2\beta),$$

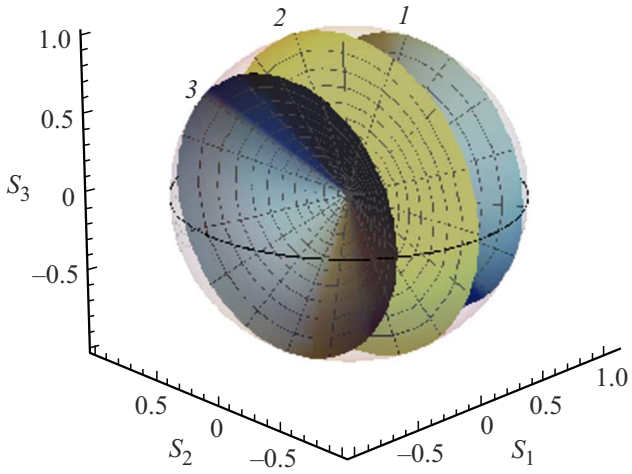

Figure 2. Behavior of the Stokes vector on the Poincare sphere in a homeotropically oriented NLC with changing electrostatic field strength ($E_s/E_{sc} = 1 - 1.2$) at fixed thickness. Azimuthal angle of incident polarization $\beta_0 = \pi/6$ (1); $\pi/4$ (2); $\pi/3$ (3). Other parameters: $\varepsilon_e = 3.22$, $\varepsilon_o = 2.43$; $\lambda = 0.5\,\mu$m, $d = 6\,\mu$m.

$$S_2(z) = \sin(2\beta)\cos\left[\frac{2\pi\sqrt{\varepsilon_0}}{\lambda}\frac{\varepsilon_a}{\varepsilon_e}\left(\frac{\varepsilon_a}{\varepsilon_e} - 1\right) \times \left(z - \frac{d}{2\pi}\sin\frac{2\pi z}{d}\right) - \delta_0\right],$$

$$S_3(z) = -\sin(2\beta)\sin\left[\frac{2\pi\sqrt{\varepsilon_0}}{\lambda}\frac{\varepsilon_a}{\varepsilon_e}\left(\frac{\varepsilon_a}{\varepsilon_a} - 1\right) \times \left(z - \frac{d}{2\pi}\sin\frac{2\pi z}{d}\right) - \delta_0\right], \qquad (8b)$$

Note the following feature of the problem. Because the propagation of components $E_x(z)$ and $E_y(z)$ is independent (see system (4)), it is clearly impossible to unambiguously represent the behavior of linear polarization inside the medium if it matches the optical axes at the input. Therefore, for a clear demonstration of the characteristics of solution (7), the incident wave polarization must be either linear with azimuth $\beta_0 \neq 0, \pi/2$ or elliptical.

4.1. Evolution of polarization in inhomogeneous anisotropic NLC

For concreteness, only the case of linear polarization is discussed. Figure 2 shows the Stokes vector behavior on the Poincare sphere at three different azimuthal angles of the incident linearly polarized wave with changing electrostatic field strength (cell thickness fixed). Similar behavior is observed in the spatial polarization state evolution at constant electrostatic field strength [17]. As seen, the Stokes vector rotates on the surface of a cone. Clearly, this Stokes vector rotation corresponds to the change in polarization state of the output wave as the electrostatic field

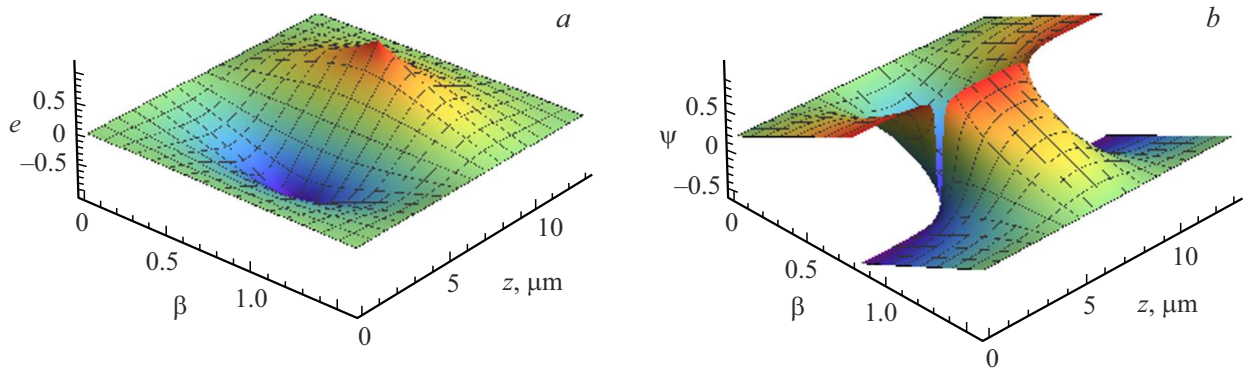

Figure 3. 3D dependence of parameters $e(z)$ and $\psi(z)$ on spatial coordinate and azimuthal angle of incident polarization ($\varepsilon_e = 3.22$, $\varepsilon_o = 2.43$; $E_{sc} \sim 1$ V/cm (for MBBA); $\lambda = 0.5\,\mu$m).

strength varies, which can be used to control the output light polarization state.

From this figure, the following conclusions can be drawn:

— The cone opening angle depends on the azimuth of the incident wave and determines the maximum possible ellipticity for a given geometry.

— Increasing the sample thickness corresponds to an increase in the number of Stokes vector rotations.

For detailed quantitative analysis, the parameters of ellipticity $e(z)$ and azimuth $\psi(z)$ are convenient; they can be expressed through the Stokes vector components as: [19]:

$$\frac{b}{a} = e(z) = \operatorname{tg}\left\{\frac{1}{2}\arcsin S_3(z)\right\};$$

$$\psi(z) = \frac{1}{2}\operatorname{arctg}\frac{S_2(z)}{S_1(z)}. \qquad (9)$$

Here a and b are the major and minor axes of the polarization ellipse, andψ is the azimuth angle — that is, the angle of the major ellipse axis with respect to the x axis.

Figs. 3, *a, b* show 3D graphs of parameters $e(z)$ and$\psi(z)$ versus spatial coordinate and incident wave polarization azimuth when anisotropy inhomogeneity is realized via the Fredericks effect. From Fig. 3, *a*, ellipticity changes smoothly, whereas azimuth behavior near angle $\pi/4$ shows a jump (Fig. 3, *b*). However, this jump is not a true discontinuity. [20]. As follows from (8b) and (9), this jump is caused by the behavior of function $\operatorname{tg} 2\beta$ near angle $\beta = \pi/4$. This is a consequence of the azimuth range being limited from$-\pi/2$ to $+\pi/2$.

To clarify the role of specific dependencies, consider a specific example — namely, the ellipticity parameter evolution $e(z)$ versus spatial coordinate in an NLC MBBA cell.

Figure 4, *a* shows this dependence for uniform (1) and inhomogeneous (2) NLC director orientations. In a homogeneous anisotropic medium, polarization beating from linear to circular and back is well known (Fig. 4, *a* curve *1*). In the inhomogeneous anisotropic case, several peculiarities arise (Fig. 4 *a*, curve *2*). Due to rigid boundary conditions, near cell surfaces, the reorientation angle varies slowly, resulting in smooth ellipticity variation. Oscillations appear in the cell interior with their number growing proportionally with sample thickness. Fig. 4, *b* shows ellipticity evolution in the inhomogeneous anisotropic medium at three different incident polarization azimuth angles.

The graphs indicate:

- Variation of incident wave azimuthal angle β_0 affects only the modulation of ellipticity oscillations,
- the maximum modulation of these parameters increases with the azimuth angle; at $\beta_0 = \pi/4$ and corresponding external field strength, the wave is circularly polarized.

It is worth emphasizing that all results are fully confirmed by direct numerical solution of the system (1). The analytical solution (9) is notable for its simplicity, clarity, and universality.

4.2. Controllable phase wafers

For practical purposes, it is more convenient to consider the dependence of the polarization state on the electrostatic field strength at fixed thickness.

For example, Fig. 5 shows ellipticity $e(E_s/E_{sc})$ and azimuth $\psi(E_s E_{sc})$ ependence on normalized applied field for three azimuthal angles of incident polarization. As seen, in an inhomogeneous anisotropic medium, polarization changes from linear to elliptical with varying electrostatic field strength. At azimuth $\beta_0 = \pi/4$ and corresponding field strength, a linearly polarized wave becomes circularly polarized ($e = 1$).

Thus, it is clear that a thin layer (at fixed thickness) of homeotropically oriented NLC can serve as a controllable phase wafer. One can estimate the minimal sample thickness corresponding to a particular output polarization state. Using (7), the phase difference δ between components

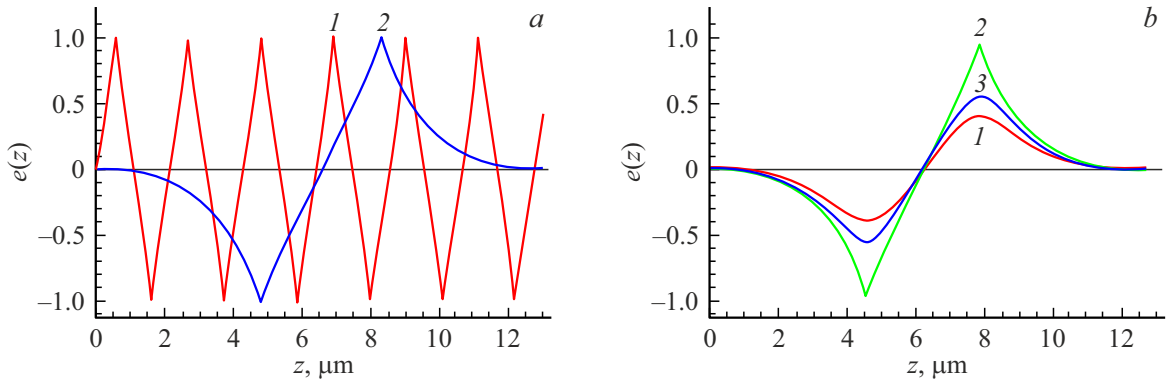

Figure 4. Dependence of ellipticity parameter $e(z)$ on spatial coordinate at thickness $d \sim 13\,\mu$m, (a) Curve 1 corresponds to uniform orientation (principal axes aligned with coordinate axes x and y), curve 2 to inhomogeneous orientation. Incident polarization azimuth $\beta_0 = \pi/4$. (b) Role of incident polarization azimuth: $\beta_0 = \pi/9$ (1); $\pi/4$ (2); $(\pi)/3$ (3). Other parameters: $\varepsilon_e = 3.22$, $\varepsilon_o = 2.43$; $E_{sc} \sim 1$ V/cm (for MBBA); $\lambda = 0.5\,\mu$m.

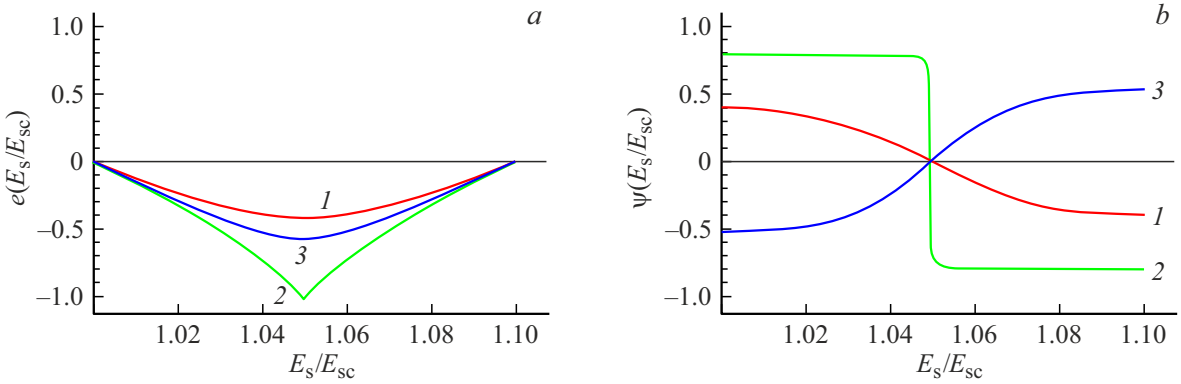

Figure 5. Dependence of azimuth angle $\beta(z)$on spatial coordinate. Incident polarization azimuth: $\beta_0 = \pi/8$ (1), $\pi/3$ (3), $\sim \pi/4$ (2). Other parameters are same as in Fig. 2.

$E_y(z)$ and $E_x(z)$ of the output wave can be estimated:

$$\delta(z) = \delta_y - \delta_x = \delta_0 - \frac{2\pi}{\lambda}\frac{\varepsilon_a\sqrt{\varepsilon_0}}{\varepsilon_e} \times \left(\frac{E_s}{E_{sc}} - 1\right)\left(z - \frac{d}{2\pi}\sin\frac{2\pi z}{d}\right). \qquad (10)$$

Let us discuss particular examples.

Quarter-wave wafer: For an incident linearly polarized wave ($\delta_0 = 0$) he output wave is circularly polarized if $\beta_0 = \pi/4$ and $\delta(d) = (2k+1)\pi/2$. From (10), the value of E_s/E_{sc} at which such an NLC cell operates as a quarter-wave plate can be calculated:

$$E_s/E_{sc} = 1 + \frac{\lambda}{4}\frac{\varepsilon_e}{\varepsilon_a\sqrt{\varepsilon_o}}\frac{2k+1}{d},$$

where k is an integer. For example, at $k = 1$ $E_s/E_{sc} \approx 1.05$, which agrees well with Fig. 5. At $k = 2$ – $E_s/E_{sc} \approx 1.15$.

Half-wave wafer: Similarly, E_s/E_{sc} can be estimated for the phase plate to act as a half-wave wafer $\lambda/2$. In this case, for incident linear polarization $\delta_0 = 0$) and $\delta(d) = \pi$ the NLC layer acts as a half-wave wafer (output wave remains linearly polarized, but the azimuth angle is rotated by $2\beta_0$, where β_0 is the incident azimuth) if

$$\frac{E_s}{E_{sc}} = 1 + \frac{\lambda}{2}\frac{\varepsilon_e}{d\varepsilon_a\sqrt{\varepsilon_o}}.$$

Substituting numerical values yields $E_s/E_{sc} \approx 1.1$), also in good agreement with Fig. 5.

5. Conclusion

This work theoretically studies the peculiarities of polarized light propagation in an inhomogeneous anisotropic NLC layer. It is shown that applying the quasi-isotropic approximation of geometric optics allows analysis from a unified viewpoint. The method is demonstrated effectively on a homeotropically oriented NLC layer under a transverse electrostatic field. A complete theoretical analysis was conducted, and convenient analytical expressions for the Stokes parameters describing the spatial evolution of the

light polarization state in a layer of such an inhomogeneous anisotropic medium were obtained. Using the derived expressions,

- the peculiarities of the evolution of the ellipticity and azimuthal angle parameters as functions of the longitudinal coordinate (at $E_s/E_{sc} = \text{const}$)),
- the issue of jump-like phase changes near the azimuthal angle $\beta_0 = \pi/4$was considered,
- the polarization behavior at the output of the LC medium with fixed thickness was analyzed; it was demonstrated that controlling the output polarization state by varying the field strength is feasible and practically convenient,
- it was shown that such a cell can operate as a phase plate of various types, in particular as quarter-wave and half-wave wafers.

Although the final analysis was performed for an NLC layer in the presence of an external static electric field, the obtained analytical expressions are sufficiently general and can be easily adapted to cases of other mechanisms inducing anisotropy inhomogeneity.

References

[1] M. Chekhova, P. Banzer. Polarization of Light. In: *Classical, Quantum, and Nonlinear Optics* (Walter de Gruyter GmbH, Berlin, Boston, 2021). DOI: 10.1515/9783110668025

[2] B.E.A. Saleh, M.C. Teich. *Fundamentals of Photonics* (John Wiley & Sons, Hoboken, 2019). DOI: 10.1002/0471213748

[3] S. Obayya, M.F.O. Hameed, N.F.F. Areed. Computational Liquid Crystal Photonics. Fundamentals, Modelling and Applicattions (John Wiley & Sons, West Sussex, 2016). DOI: 10.1002/ 9781119041993

[4] Sh. Xu, F. Fan, Sh. Chen, Y. Xing, Y. Gao, H. Li, G. Niu, Sh. Chang. Optical Materials Express, **11**, (1), 171 (2021). DOI:10.1364/OME.414845

[5] E. Stoyanova, S. Ivanov, A. Rangelov. Appl. Opt., **59**, 10224 (2020). DOI: 10.1364/ AO.404150

[6] X. Zhang, F. Fan, C. Zhang, Y. Ji, X. Wang, S. Chang. Optical Materials Express, **10** (2), 282 (2020). DOI: 10.1364/OME.383058

[7] Cho-Fan Hsieh, Chan-Shan Yang, Fang-Cih Shih, Ru-Pin Pan, Ci-Ling Pan. Opt. Express, **27** (7), 9933 (2019). DOI: 10.1364/OE.27.009933

[8] E. Stoyanova, M. Al-Mahmoud, H. Hristova, A. Rangelov, E. Dimova, N.V. Vitanov. J. Opt., **21**, 105403 (2019). DOI: 10.1088/2040-8986/ab40fc

[9] E.V. Aksenova, A.A. Karetnikov, N.A. Karetnikov, A.P. Kovshik, A.V. Svanidze, S.V. Ul'yanov. Nanosystems: Phys. Chem. Math., **14** (1), 74 (2023). DOI: 10.17586/2220-8054-2023-14-1-74-85

[10] E.V. Aksenova, A.A. Karetnikov, N.A. Karetnikov, A.P. Kovshik, E.I. Ryumcev, A.S. Sahackij, A.V. Svanidze. ZhETF, **149** (5), 1087 (2016) (in Russian). DOI: 10.7868/ S0044451016050175

[11] Yu.A. Kravtsov. Geometrical Optics in Engineering Physics (Alpha Science, London, 2005).

[12] B. Bieg, J. Chrzanowski, Yu. A.Kravtsov, F. Orsitto. Physics Procedia, **62**, 102 (2015). DOI: 10.1016/j.phpro.2015.02.018

[13] H. Kubo, R. Nagata. JOSA, **73** (12), 1719-1724 (1983).

[14] A.L. Aslanyan, L. Aslanyan, Yu.S. Chilingaryan. Opt. Spectrosc., **116**, 483 (2014).

[15] L.S. Aslanyan, H.H. Hovakimyan. JOSA B, **37** (3), 847 (2020). DOI: 10.1364/ JOSAB.378809

[16] L.S. Aslanyan, A.E. Ayvazyan. J. Contemporary Physics (Armenian Academy of Sciences), **58**, 59 (2023). DOI: 10.54503/0002-3035-2023-58.1-84

[17] L.S. Aslanyan, A.E. Ajvazyan. Opt. i spektr., bf 130 (8), 1174−1180 (2022). (in Russian) DOI: 10.21883/OS.2022.08.52903.3295-22

[18] P.G. De Gennes, J. Prost. *The Physics of Liquid Crystals,* 2nd ed. (Clarendon Press., Oxford, 1993). DOI: 10.1063/1.2808028

[19] D.H. Goldstein. *Polarized Light*, 3rd ed. (CRC Press, Boca Raton, 2017). DOI: 10.120 1/b10436

[20] R.M.A. Azzam, B.E. Merrill, N.M. Bashara. Appl. Opt., **12** (4), 764 (1973). DOI: 10.1364/AO.12.000764

Translated by J.Savelyeva